Brain Struct Funct (2014) 219:1587–1601
DOI 10.1007/s00429-013-0587-6

ORIGINAL ARTICLE

Organization and chemical neuroanatomy of the African elephant (*Loxodonta africana*) hippocampus

Nina Patzke · Olatunbosun Olaleye · Mark Haagensen · Patrick R. Hof · Amadi O. Ihunwo · Paul R. Manger

Received: 22 April 2013 / Accepted: 22 May 2013 / Published online: 2 June 2013

Abstract Elephants are thought to possess excellent long-term spatial–temporal and social memory, both memory types being at least in part hippocampus dependent. Although the hippocampus has been extensively studied in common laboratory mammalian species and humans, much less is known about comparative hippocampal neuroanatomy, and specifically that of the elephant. Moreover, the data available regarding hippocampal size of the elephant are inconsistent. The aim of the current study was to re-examine hippocampal size and provide a detailed neuroanatomical description of the hippocampus in the African elephant. In order to examine the hippocampal size the perfusion-fixed brains of three wild-caught adult male African elephants, aged 20–30 years, underwent MRI scanning. For the neuroanatomical description brain sections containing the hippocampus were stained for Nissl, myelin, calbindin, calretinin, parvalbumin and doublecortin. This study demonstrates that the elephant hippocampus is not unduly enlarged, nor specifically unusual in its internal morphology. The elephant hippocampus has a volume of 10.84 ± 0.33 cm^3 and is slightly larger than the human hippocampus (10.23 cm^3). Histological analysis revealed the typical trilaminated architecture of the dentate gyrus (DG) and the cornu ammonis (CA), although the molecular layer of the dentate gyrus appears to have supernumerary sublaminae compared to other mammals. The three main architectonic fields of the cornu ammonis (CA1, CA2, and CA3) could be clearly distinguished. Doublecortin immunostaining revealed the presence of adult neurogenesis in the elephant hippocampus. Thus, the elephant exhibits, for the most part, what might be considered a typically mammalian hippocampus in terms of both size and architecture.

Keywords Adult hippocampal neurogenesis · Calcium-binding proteins · Hippocampus · Doublecortin · Memory · Proboscidean

N. Patzke · O. Olaleye · A. O. Ihunwo · P. R. Manger (✉)
School of Anatomical Sciences, Faculty of Health Sciences, University of the Witwatersrand, 7 York Road, Parktown, Johannesburg 2193, South Africa
e-mail: Paul.Manger@wits.ac.za

M. Haagensen
Department of Radiology, Donald Gordon Medical Centre, University of the Witwatersrand, Parktown, Johannesburg 2193, South Africa

P. R. Hof
Fishberg Department of Neuroscience and Friedman Brain Institute, Icahn School of Medicine at Mount Sinai, One Gustave L. Levy Place, New York, NY 10029, USA

Introduction

The African elephant is the largest terrestrial mammal with a brain mass of approximately 5 kg (Shoshani et al. 2006; Manger et al. 2009). Field observations have demonstrated that African elephants rely on the long-term spatial memories of older individuals, sometimes travelling hundreds of kilometres in search of long unused food and water resources (Byrne et al. 2009; Hart et al. 2008). Indeed, groups with older individuals were found to have better chances of survival during long drought periods, potentially relying on the memories of the older members of the herd to locate sufficient supplies of food and water (Foley et al. 2008; Byrne et al. 2009; Hart et al. 2008). In contrast, groups of younger elephants, lacking this experience, had smaller geographic ranges and had an overall higher mortality rate during drought periods (Foley et al. 2008).

Elephants are social animals, many of which live in matriarchal family groups numbering between around 20 related individuals, however, these smaller family groups can come together to form a "super-herd" sometimes consisting of related and unrelated individuals numbering over 400 (Western and Lindsay 1984) when social greetings, both auditory and tactile, are readily observed (Vidya and Sukumar 2005; Poole et al. 1988). In contrast, adult male elephants often lead a solitary life (Skinner and Chimimba 2005). For the stability of a large and flexible social group such as seen in African elephants it is important for the individuals within a group to be able to learn to identify and remember other individuals. Chemosensory experiments with urine samples of conspecifics have demonstrated that elephants can recognize and memorize up to 17 different females and up to 30 family members (Bates et al. 2008). In addition, elephants are capable of recognizing family members as opposed to unfamiliar elephants due to the individual acoustic characteristics of their vocalizations (McComb et al. 2003). It has also been shown that elephants can recognize the calls of approximately 100 other elephants from various families and clans (McComb et al. 2000), providing strong evidence for an extensive social memory.

Both spatial and social memories appear, at least in part, to be hippocampus dependent. Lesion and immediate early gene experiments, as well as single cell recording, provide a large body of evidence that spatial memory, or more specifically navigation through space using cognitive maps, is hippocampus dependent (Morris 2007); however, the role of the hippocampus in social memory is ambiguous. Neuronal recordings in humans suggest that the hippocampus responds to individuals (Quiroga et al. 2005) and hence might be involved in social memory, while studies in rodents argue against the possible role of the hippocampus in social memory (e.g. von Heimendahl et al. 2012).

Recently the gross anatomy of the elephant hippocampus has been reported in two studies (Hakeem et al. 2005; Shoshani et al. 2006). Hakeem et al. (2005) using MRI scans of a single female African elephant with a brain significantly smaller than the average adult elephant brain (4 kg compared with the average being closer to 5 kg), reported that the hippocampus of the elephant was very large; however, it would appear from the images provided by Hakeem et al. (2005) that they were including a large portion of the occipital pole cortex in their non-quantitative estimation of hippocampal volume. In contrast, Shoshani et al. (2006), who examined the hippocampus from seven adult elephants from both the African ($n = 4$) and Asian ($n = 3$) species, reported a hippocampus similar in size to that of humans (which is 10.23 cm^3, Stephan et al. 1981); however, neither study reported a specific volume for the elephant hippocampus, making any inference about hippocampal volume and memory in the elephant difficult to interpret. To the authors' knowledge, only one study briefly reports on the internal neuroanatomical appearance of the elephant hippocampus, providing one image that indicates that the cellular structure of the elephant hippocampal anatomy is typically mammalian (Kupsky et al. 2001).

Due to the paucity of the literature regarding the elephant hippocampus, and as we have access to perfusion-fixed brain specimens of African elephant amenable to modern neuroanatomical techniques (Manger et al. 2009; Ngwenya et al. 2011; Maseko et al. 2013), we undertook to quantify the size of the elephant hippocampus of three wild-caught adult male African elephants, aged 20–30 years using MRI scans and provide the first detailed neuroanatomical description of the elephant hippocampus using immunohistochemical staining for the calcium-binding proteins parvalbumin, calbindin, and calretinin. We also provide data concerning the immunostaining pattern of the endogenous marker doublecortin (DCX), which is expressed in neuronal precursor cells and immature neurons (Brown et al. 2003; Rao and Shetty 2004), to examine adult neurogenesis in the dentate gyrus of the hippocampus. Our findings are interpreted in the functional context of reports regarding elephant memory capabilities.

Materials and methods

Specimens

The hippocampi of three adult male African elephants (LA1, LA2 and LA3), aged 20–30 years, were analyzed in the current study. Acquisition, fixation and storage of the tissue have been described previously (Manger et al. 2009). The harvesting and use of these specimens for scientific research was approved by the Zimbabwe Parks and Wildlife Management Authority, the Malilangwe Trust, and the University of the Witwatersrand Animal Ethics Committee (2008/36/1).

Magnetic resonance imaging (MRI)

Brains from the three African elephants underwent MRI to obtain measurements of hippocampal volume. The specimens were scanned on a Philips 1.5 T Intera System (Eindhoven, The Netherlands), using all three elements of the head and neck coil. The brains were removed from their storage containers (Manger et al. 2009), drained of excess fluid and placed in the head coil wrapped in a dry sheet, thus being exposed directly to air, which also partly entered the ventricles. After testing different scan parameters, the following sequence was selected as giving the best detail

and the least artefact (especially at air–fluid interfaces). The selected T1-weighted inversion recovery sequence consisting of 2 mm slices without gap, had a time to repeat between 6.5 and 10.9 s depending on the number of slices, a time to echo 10 ms and a time to invert 300 ms. The number of signal averages varied between 3 and 4 with a flip angle of 90° and an echo train of 10. The scan times varied between 15 and 25 min. The antifreeze liquid in which the brains were stored showed high signal on both T1- and T2-weighted sequences and the routine clinical T1 and T2 sequences produced very similar T2-like images of the brain specimens. This is possibly related to the lack of water in the tissues of the specimen secondary to the fixation and storage process. The images were processed using the freely available open source software program OsiriX (Rosset et al. 2004; www.osirix-viewer.com).

Calculating hippocampal volumes from MR images

For outlining the boundaries of the hippocampus we made used of the gross anatomical description provided by Shoshani et al. (2006), as well as personal experience and our observations of the histological sections made during the course of this study. We followed the anatomical delineation of the hippocampus as described by Reep et al. (2007) where the regions included in our measurement of the hippocampus included the dentate gyrus, cornu ammonis, alveus, hippocampal commissure, and the fornix-fimbria caudal to the septum. Once the hippocampal outline was defined the total hippocampal volume was calculated by multiplying the sum of the areas outlined by the MRI section thickness (2 mm).

Histological analysis

From each elephant blocks of hippocampal tissue were dissected in a plane orthogonal to the ventricular surface of the hippocampus at approximately the middle portion of the hippocampus. Each tissue block was cryosectioned into 50-µm-thick sections on a freezing microtome. Consecutive sections were stained for Nissl substance, reacted for myelin, and immunohistochemically for parvalbumin (PV), calbindin (CB), calretinin (CR), and doublecortin (DCX). The first section of each series was mounted on 0.5 % gelatine-coated slides, dried overnight, cleared in a 1:1 mixture of 100 % ethanol and 100 % chloroform and stained with 1 % cresyl violet. The second section of each series was mounted on 1 % gelatine-coated slides, dried and then stained with a modified silver stain to reveal myelinated structures (Gallyas 1979).

The sections used for free-floating immunohistochemical staining were treated for 30 min in an endogenous peroxidise inhibitor (49.2 % methanol: 49.2 % 0.1 M PB: 1.6 of 30 % hydrogen peroxide) followed by three 10 min rinses in 0.1 M PB. To block unspecific binding sites the sections were then pre-incubated for 2 h, at room temperature, in blocking buffer (3 % normal goat serum (NGS) for CB, CR, PV sections or 3 % normal rabbit serum (NRS) for DCX sections, 2 % bovine serum albumin, BSA, and 0.25 % Triton X-100 in 0.1 M PB). Thereafter sections were incubated in the primary antibody solution, made up of the appropriate dilution of the primary antibody in blocking buffer for 48 h at 4 °C under gentle agitation. Anti-calbindin (CB38a, Swant, raised in rabbit), anti-parvalbumin (PV28, Swant, raised in rabbit) and anti-calretinin (7699/3H, Swant, raised in rabbit), all at a dilution of 1:10,000, were used to reveal neuronal structures expressing these calcium-binding proteins. To examine adult neurogenesis we used the endogenous marker doublecortin (DCX), which is a microtubule-associated phosphoprotein, and is expressed in actively dividing neuronal precursor cells and their neuronal daughter cells for up to 2–3 weeks. The expression of DCX is downregulated after approximately 2 weeks, with the onset of the expression of NeuN, a marker for mature neurons (Brown et al. 2003; Rao and Shetty 2004). The visualization of DCX positive neurons also provides an average of the rate of expression of new neurons in natural conditions prior to capture of the animal (Bartkowska et al. 2010). To visualize DCX we used the goat-anti DCX SC-18 primary antibody from Santa Cruz at a dilution of 1:300. The primary antibody incubation was followed by three 10-min rinses in 0.1 M PB and the sections were then incubated in a secondary antibody solution (1:1,000 dilution of biotinylated anti-goat IgG, BA 5000, Vector Labs, for DCX sections or biotinylated anti-rabbit IgG, BA 1000, Vector Labs, in a blocking buffer containing 3 % NGS/NRS and 2 % BSA in 0.1 M PB) for 2 h at room temperature. This was followed by three 10-min rinses in 0.1 M PB, after which sections were incubated for 1 h in an avidin–biotin solution (1:125; Vector Labs), followed by three 10-min rinses in 0.1 M PB. Sections were then placed in a solution containing 0.05 % 3,3′-diaminobenzidine (DAB) in 0.1 M PB for 5 min, followed by the addition of 3.3 µl of 30 % hydrogen peroxide per 1 ml of DAB solution. Chromatic precipitation was visually monitored under a low power stereomicroscope. Staining continued until such time that the background stain was at a level that would allow for accurate architectonic matching to the Nissl and myelin sections without obscuring the immunoreactive structures. Development was arrested by placing sections in 0.1 M PB for 10 min, followed by two more rinses in this solution. Sections were then mounted on 0.5 % gelatine-coated glass slides, dried overnight, dehydrated in a graded series of alcohols, cleared in xylene and coverslipped with Depex. To ensure non-specific staining of the immunohistochemical protocol, we ran tests on sections where we omitted the

primary antibody, and sections where we omitted the secondary antibody. In both cases no staining was observed. Digital photomicrographs were captured using Zeiss Axioshop and Axiovision software. No pixelation adjustments or manipulation of the captured images were undertaken, except for the adjustment of contrast, brightness, and levels using Adobe Photoshop 7.

Results

Hippocampal volumes in the African elephant

As reported by Shoshani et al. (2006), who provided a thorough description of the gross anatomy of the elephant hippocampal formation, we observed the hippocampus to lie in the floor of the temporal horn of the lateral ventricle and the borders of the hippocampus were readily evident in all three planes scanned for MR imaging (Figs. 1, 2, 3). Volumetric MRI analysis revealed that the African elephant hippocampus has an average volume of 10.84 ± 0.33 cm^3. The three individual elephants had brain volumes and hippocampal volumes of 4,966.22 and 11.21 cm^3 (LA1), 5,067.57 and 10.73 cm^3 (LA2), and 4,666.99 and 10.57 cm^3 (LA3).

Histological analysis

Histological analysis of the elephant hippocampus revealed the typical trilaminated architecture of the dentate gyrus (DG) and the cornu ammonis. The three main subdivisions of the cornu ammonis (CA1, CA2 and CA3) could be clearly distinguished (Fig. 4).

Dentate gyrus

The dentate gyrus (DG) of the African elephant was comprised of three layers. The molecular layer (ML) and the granule layer (GL) form roughly a U-shaped structure, but in the elephant hippocampus, these layers of the dentate gyrus exhibit two additional folds when compared to most other mammals. The molecular and granule layers enclosed the polymorphic layer (PL).

The ML was the most superficial layer, being closest to the hippocampal fissure, and is a neuron sparse layer. Three differently shaped neuronal types could be identified in the Nissl-stained sections, and these were mostly located in the deeper half of the ML. The neurons present in the ML had somata that were either oval or triangular in shape, with the occasional fusiform-shaped soma located in close proximity to the GL (Fig. 5a). These neurons showed no immunoreactivity to parvalbumin, calbindin (Fig. 5c, d) or calretinin. Myelin staining revealed a relatively dense myelinated fibre network (Fig. 5b). Interestingly, the myelinated fibres were not evenly distributed in the ML, but rather the deeper half of the ML, close to the GL, had a higher myelin density than the superficial half of the ML, allowing the delineation of a myelin dense inner (iML) and a myelin sparse outer molecular layer (oML). This sublamination was even more impressive in the calretinin-stained sections. In both the iML and oML, a deep to superficial gradient of calretinin immunoreactivity was observed. In this case, for both sublamina of the molecular layer, the deeper portions of the lamina revealed the highest calretinin neuropil labelling which became less intense until no calretinin staining was visible at the most superficial level of each sublamina (Figs. 4f, 5d). In contrast to the heterogenous calretinin immunolabelling of the ML, calbindin immunolabelling revealed a homogenous neuropil with a moderate staining intensity. Only a few parvalbumin positive fibres were observed in the iML.

The granule layer (GL), which lies deep to the iML, consisted mostly of densely packed elliptical-shaped granule cells, the principal neurons of the dentate gyrus. At its deepest extent the GL had a depth of approximately 15 granule cells, while at its thinnest the GL had a depth of approximately 5 cells (Fig. 5a). The depth of the GL appeared to be dependent on the angle at which the layer was sectioned. At the border between the GL and ML neurons with an oval-shaped soma were present. The myelin density in the GL was very low and revealed a loose network of mostly radially oriented fibres (Fig. 5b). Calbindin was strongly expressed in granule cells and their processes (Fig. 5c), which give rise to the mossy fibres that project to the pyramidal cells of the pyramidal layer in CA3 (Figs. 4f, 6d). A sparse calretinin-immunopositive terminal network was observed in the GL, as well as a sparse number of parvalbumin-immunopositive fibres.

The polymorphic layer was the deepest layer observed within the DG. The PL contained a moderate number of diffusely arranged neurons exhibiting different soma shapes, and these neurons were larger than those in the GL and ML. Nissl staining revealed numerous oval, triangular and multipolar, as well as occasional fusiform neuronal soma, while myelin staining revealed a high density of myelinated fibres throughout this layer (Fig. 5a). A moderately dense calbindin-immunopositive terminal network was seen throughout this layer, but only a modest number of calretinin-immunopositive processes (Fig. 5c) and the occasional parvalbumin-immunopositive fibres were observed. Calretinin immunostaining revealed a moderate number of weakly to moderately immunostained neurons that had three to four thick dendrites emanating from the triangular or multipolar-shaped soma (Fig. 5d). These neurons were presumably hilar mossy cells. No parvalbumin- or calbindin-immunopositive neurons were observed.

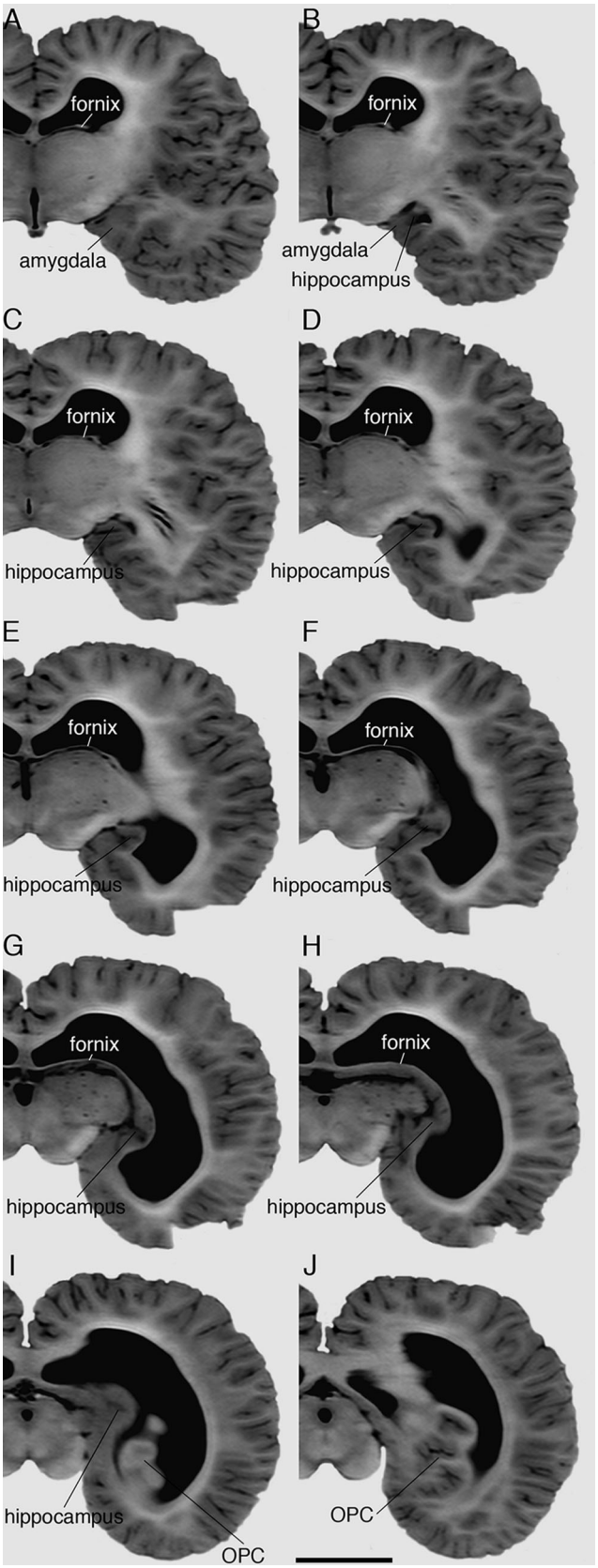

◀**Fig. 1** Coronal MR images of the elephant brain showing the size and position of the hippocampus. **a**–**j** Sequence of rostral to caudal 2-mm-thick slices that are 4 mm apart. *Scale bar* in **j** = 5 cm and applies to all. *OPC* occipital pole cortex

Cornu ammonis (CA)

The cornu ammonis (CA) could be divided into three distinct architectural fields: CA3, CA2 and CA1. All three fields revealed the typical three layered organization and could be subdivided into following layers: the polymorphic layer or stratum oriens (SO), the stratum pyramidale (SP) and the plexiform layer. The plexiform layer could further be subdivided into the stratum lucidum (SL, only in CA3), stratum radiatum (SR) and stratum lacunosum moleculare (SLM) (Fig. 4).

The stratum oriens (SO), the deepest layer, was a relatively neurons sparse layer. Nissl staining revealed neurons mostly located close to the border of SO with SP (Fig. 6a, e, i).

These neurons had somata that were oval, stellate, or fusiform in shape. The fusiform-shaped neurons were oriented horizontally, were mainly located in the CA1 field and were immunopositive for parvalbumin, calbindin and calretinein (Fig. 6d, h). Myelin staining in this layer revealed a mostly uniform dark stain due to the high density of myelinated axons. Superficially in the SO individual myelinated fibres were visible. Sparse calbindin and calretinin and a modest parvalbumin-immunopositive terminal networks were observed in the SO.

The stratum pyramidale (SP) consisted of pyramidal cells, these being the principal neurons of the hippocampus (Fig. 6a, e, i). The superficial aspect of the SP was clearly marked by compactly arranged pyramidal cells. Towards the SO the pyramidal cells became more loosely arranged. The cellular band of the CA3 field was less dense towards the DG and became more densely packed towards CA2. The pyramidal cells were most densely packed at the border of CA3 and CA2. The cellular band in the CA1 field was broader than in CA3 and CA2 and became even broader towards the transition to the subiculum. Here again, the cells at the superficial aspect of the SP were more densely packed than the cells toward the SO, which made it difficult to define an exact border between the SP and SO. Immunostaining with the anti-parvalbumin antibody revealed a moderate number of immunopositive neurons and processes in the CA3 (Fig. 6c) and CA2 (Fig. 6g) fields with a progressive decrease in parvalbumin-immunopositive neuronal number towards the CA1 field. Most of these neurons were pyramidal in shape and had two basal dendrites that extended into SO and an apical dendrite that extended into SR and SLM. Only a few calretinin-immunopositive

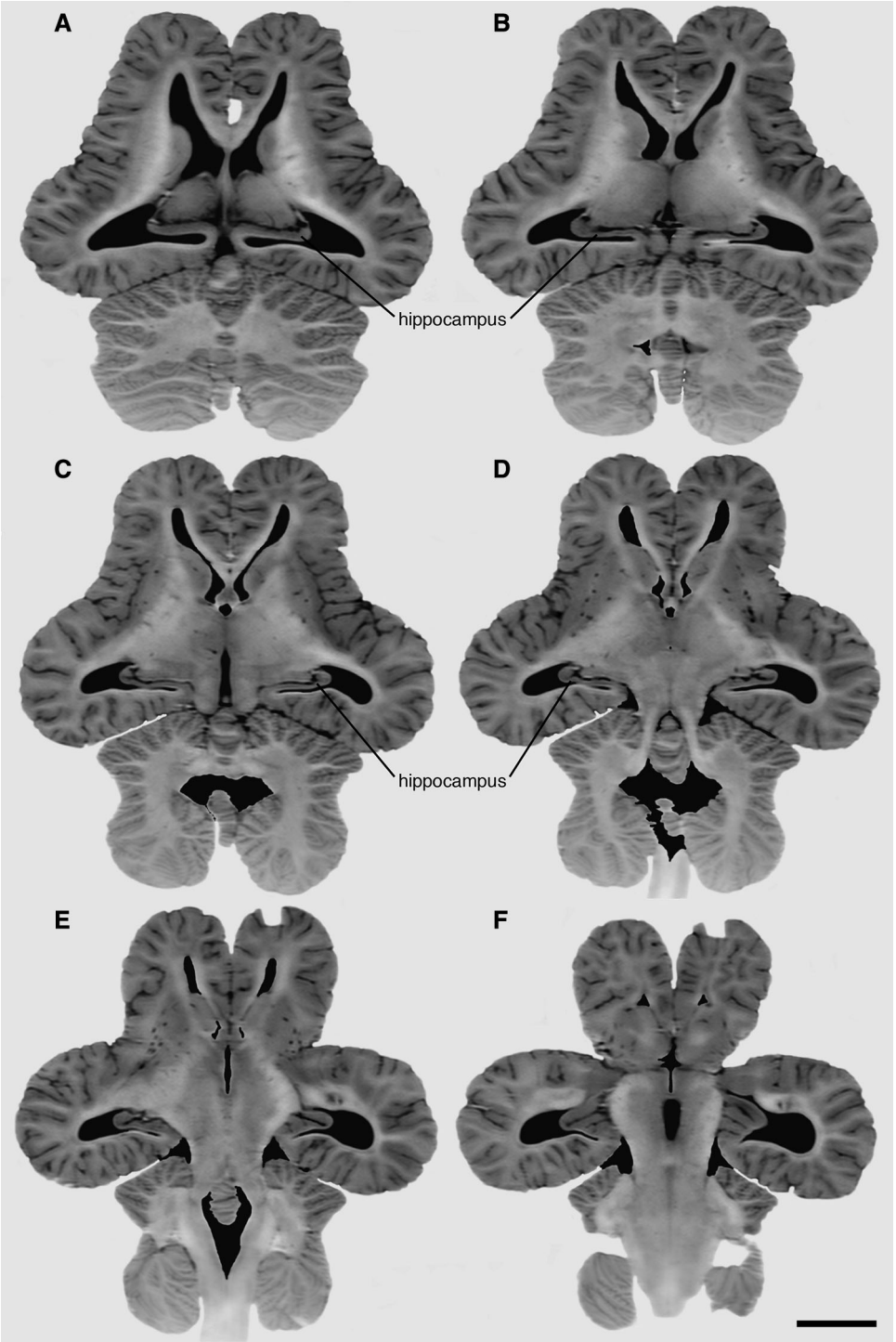

Fig. 2 Horizontal MR images of the elephant brain showing the size and position of the hippocampus. **a**–**f** Sequence of dorsal to ventral 2-mm-thick slices that are 8 mm apart. *Scale bar* in **f** = 5 cm and applies to all

neurons could be observed in the CA3 field, presumably interneurons, as they had soma that were either oval or stellar in shape and were mostly located in the deeper half of the layer. Occasional calbindin-immunopositive neurons were observed in the CA3 (Fig. 6d) and CA2 (Fig. 6h) field. Myelin staining in this layer revealed a network of loosely arranged myelinated fibres throughout all three CA fields (Fig. 6b, d, j).

Within the plexiform layer of the three CA fields, two distinct strata could be identified, these being the stratum radiatum (SR) and the stratum lacunosum moleculare (SLM) with the SLM being the most superficial sublamina. In addition, the CA3 field had an extra sublamina, the stratum lucidum (SL), which contained the mossy fibres of the granule cells of the DG, and was located between the SP and SR in the CA3 field. The presence of the SL was a

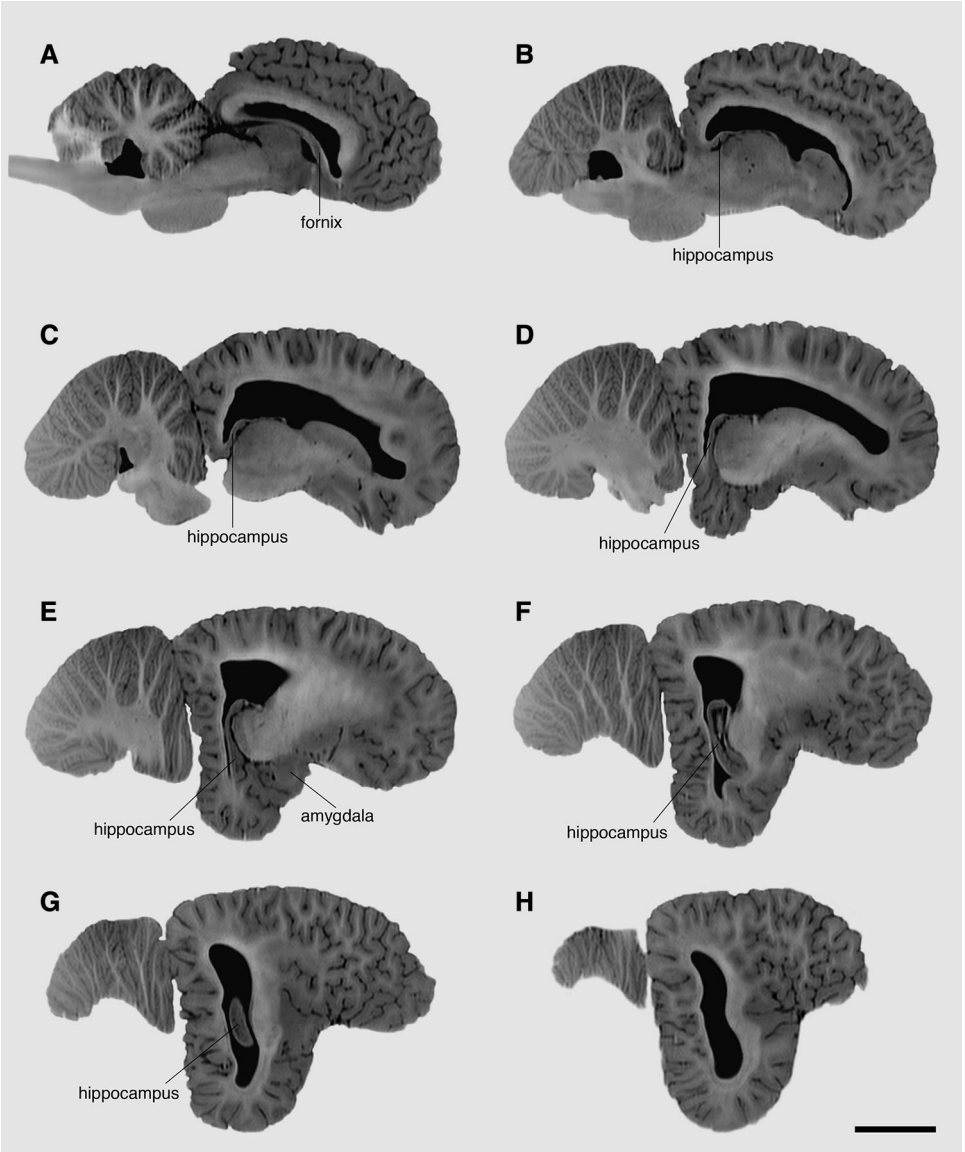

Fig. 3 Sagittal MR images of the elephant brain showing the size and position of the hippocampus. **a**–**h** Sequence of medial to lateral 2-mm-thick slices that are 4 mm apart. *Scale bar* in **h** = 5 cm and applies to all

reliable marker of the border between CA3 and CA2. The SL could not be distinguished from the other layers in Nissl- or myelin-stained sections, and showed no immunoreactivity for parvalbumin and calbindin; however, the SL was clearly visible in calbindin-stained sections, which revealed the calbindin-immunopositive mossy fibres of the granule cells of the DG (Fig. 6d). In close proximity to the dentate gyrus the mossy fibres were found to run above, within and below the pyramidal layer. Towards the mid portion of CA3 the mossy fibres ran above and within the PL, but the fibres running with the PL waned with distance from the DG, and only the bundle that ran superficial to the PL remained to occupy the SL.

The SR was located superficial to the SL in the CA3 field and superficial to the SP in the CA2 and CA1 fields, and across all three fields the SLM was found superficial to the SR. Both sublamina were relatively cell sparse. In Nissl-stained sections a few neurons of different shapes could be observed as well as some displaced pyramidal cells; however, more neurons were observed in the SR than in the SLM (Fig. 6a, e, i). These neurons exhibited soma that were either oval, triangular, multipolar or fusiform in shape and that were smaller in size than the pyramidal cells of the SP. Parvalbumin immunoreactivity revealed a few multipolar- and triangular-shaped neuronal somata in the SR, whereas calretinin immunostaining revealed both bipolar and multipolar cells in the SR and SLM. In the SR myelin staining was moderately dense and consisted of myelinated axons showing no particular orientation, but in the more superficial SLM, the myelin staining was more intense and consisted mostly of tangentially oriented fibres (Fig. 6b, f, j). A dense parvalbumin-immunopositive terminal network was

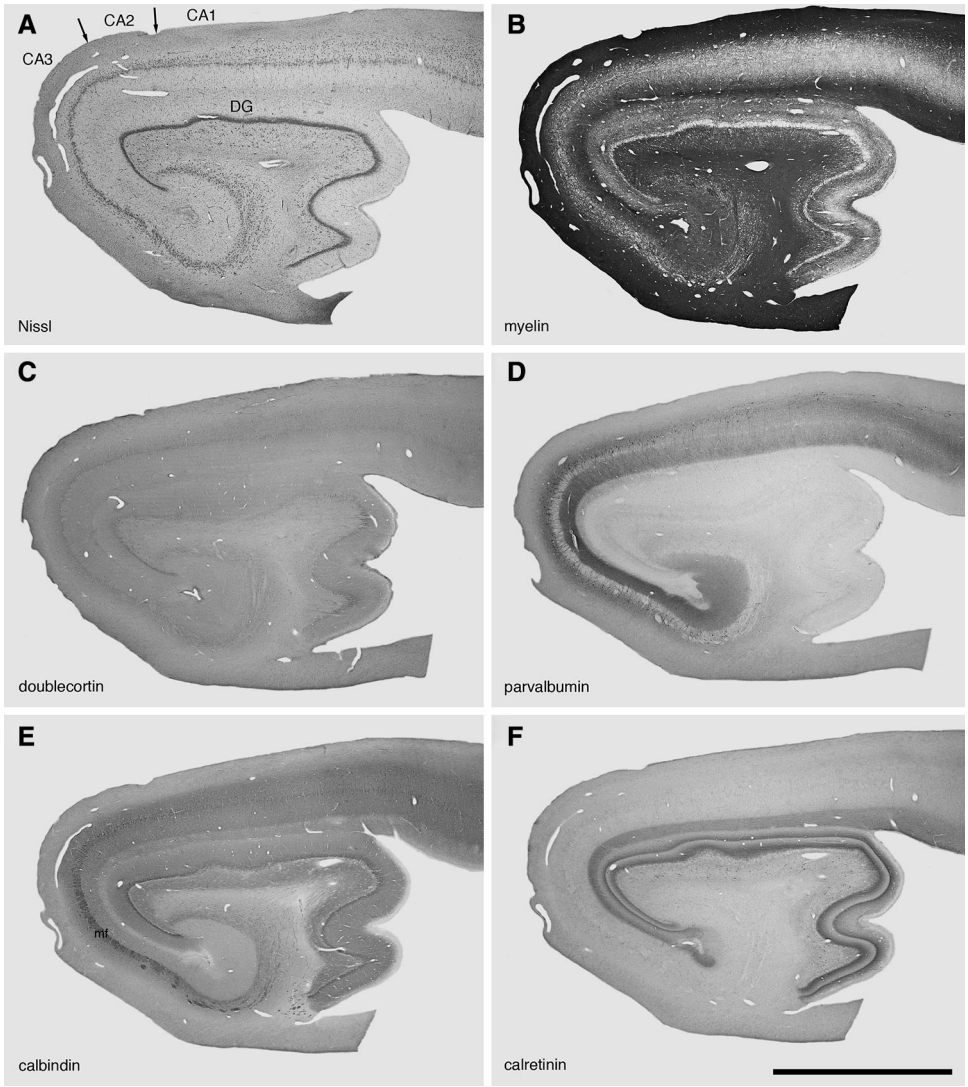

Fig. 4 Low-power photomicrographs of the elephant hippocampus. The elephant hippocampus revealed the typical trilaminated architecture of the dentate gyrus (DG) and the cornu ammonis (CA). Three main subdivisions of the cornu ammonis (CA1, CA2 and CA3) could be clearly distinguished. The border between CA3 and CA2 was clearly marked by the presence of calbindin-immunopositive mossy fibres (mf). The borders of CA3 with CA2 and CA2 with CA1 are marked by *arrows* (**a**). **a** Nissl stain, **b** myelin stain, **c** DXC immunostain, **d** parvalbumin immunostain, **e** calbindin immunostain, **f** calretinin immunostain. *Scale bar* in **f** = 5 mm and applies to all

observed in the SR of the CA3 (Fig. 6c) and CA2 (Fig. 6g) fields, but the parvalbumin-immunopositive terminal network was less dense in CA1 and became progressively less dense until it disappeared at the CA1/subiculum border. A sparse parvalbumin-immunoreactive terminal network was observed in the SML in the CA3 (Fig. 6c) and CA2 (Fig. 6g) fields, but this was not present within the CA1 field. A moderate number of calbindin-immunopositive fibres were observed in both the SR and SLM, but a higher density was seen in the SR (Fig. 6d, h, l). Calretinin immunostaining revealed a moderately dense terminal network in the SLM, with the occasional occurrence of individual tangentially oriented processes.

Evidence for adult neurogenesis in the elephant dentate gyrus

Evidence for adult neurogenesis in the dentate gyrus of the elephant was provided by immunostaining for doublecortin (DCX). A moderate density of DCX-immunopositive neurons was observed in the subgranular zone (SGZ) of the granule layer and at the basal end of the granule layer of the DG (Fig. 7). These neurons had soma that were elliptical in shape and extended their dendrites into the ML of the DG. A few DCX-immunopositive processes were observed in the polymorphic layer, presumably mossy fibres of the newly generated neurons located in the granule layer.

Discussion

The current study contributes substantial quantitative and qualitative information to previous observations made on the size and morphology of the hippocampus in the African elephant. We found that the elephant hippocampus exhibits a range of features that are typical among mammals in terms of the size of the hippocampus and the laminar and

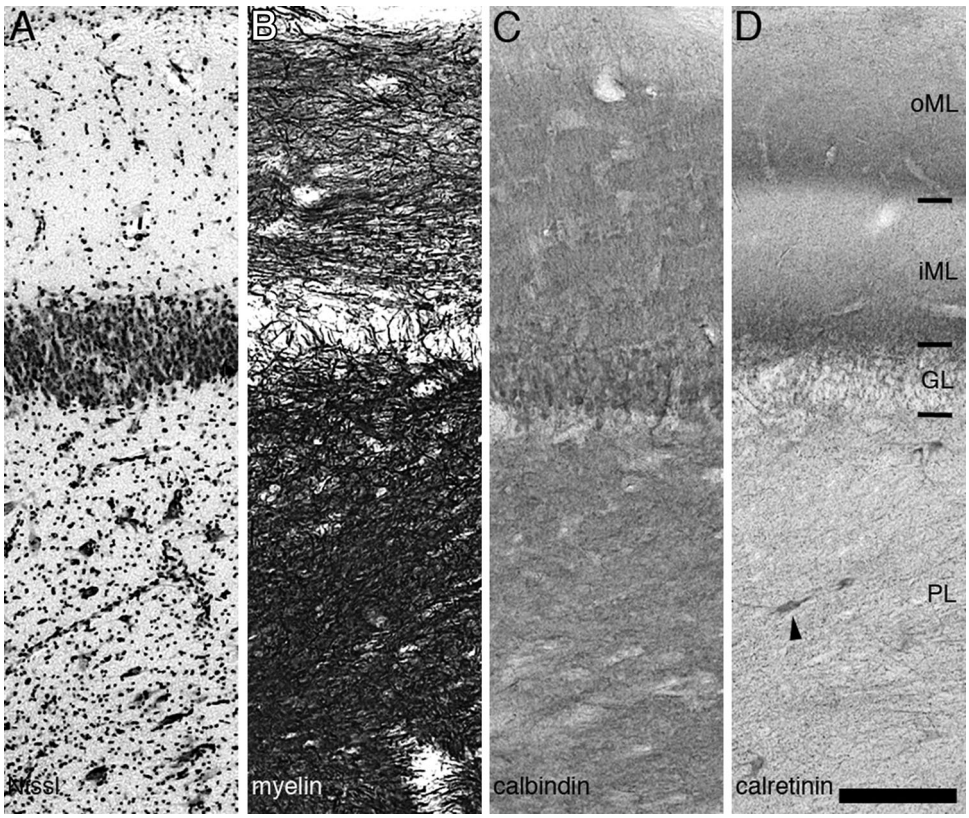

Fig. 5 Higher power photomicrographs of the dentate gyrus. The dentate gyrus could be subdivided in the polymorphic layer (PL), the granule cell layer (GL) and the outer and inner molecular layers (oML and iML). **a** Nissl staining revealed a cell dense GL and a neuron sparse ML and PL. **b** A dense myelinated fibre network was observed in the ML and PL. **c** Densely packed, calbindin-immunoreactive granule cells were observed in the GL as wells as their processes in the ML and PL. **d** Calretinin immunostaining revealed a moderate number of neurons that had three to four thick dendrites emanating from the triangular or multipolar-shaped soma, presumably hilar mossy cells (see *arrow*) in the PL. In the ML two deep to superficial gradient of calretinin immunoreactivity were observed, subdividing it into an outer (oML) and inner (iML) molecular layer. *Scale bar* in **d** = 250 μm and applies to all

cellular organization of this structure. The apparent circuitry and neurochemistry of some aspects of the neurons also reveal a phenotype that did not show any major departure compared to previous observations in other mammals. The one major difference observed was in the complex sublamination of the molecular layer of the dentate gyrus as revealed with calretinin immunostaining. This difference in comparison to other mammalian species is contextualized in terms of the functional aspects of the relative and absolute size, and the apparent circuitry of the elephant hippocampus.

The volume of the elephant hippocampus

In the current study we provide the first quantification of the absolute size of the elephant hippocampus. In the three adult male African elephants examined, an average hippocampal volume of 10.84 cm^3 was found. This volume of the elephant hippocampus is slightly larger than the human hippocampus that has a reported volume of 10.23 cm^3 (Stephan et al. 1981) and 10.16 cm^3 (Watson et al. 1992). Our quantification is in agreement with the statement made by Shoshani et al. (2006, p. 138): "The elephant HC is approximately of the same size as the human HC, but is small relative to the overall size of the elephant cerebrum." The elephant hippocampus is in fact, approximately 0.6 cm^3 larger than the human hippocampus, but it is likely that interindividual variation in hippocampal volume within humans and elephants would make any small distinction in size insignificant. Thus, in 10 elephants examined (3 in the current study and 7 in the study of Shoshani et al. 2006), the conclusion reached is that the elephant hippocampus is not significantly larger than the human hippocampus.

In contrast to this general agreement, the study of a single female elephant with a smaller than average adult brain size (whole brain volume of 3,886.7 cm^3 Hakeem et al. 2005, p. 1117), led the authors of that study to conclude that: "the elephant has an unusually large and convoluted hippocampus compared to primates and especially cetaceans." This paper also contains other unusual statements regarding hippocampal size in Afrotherians,

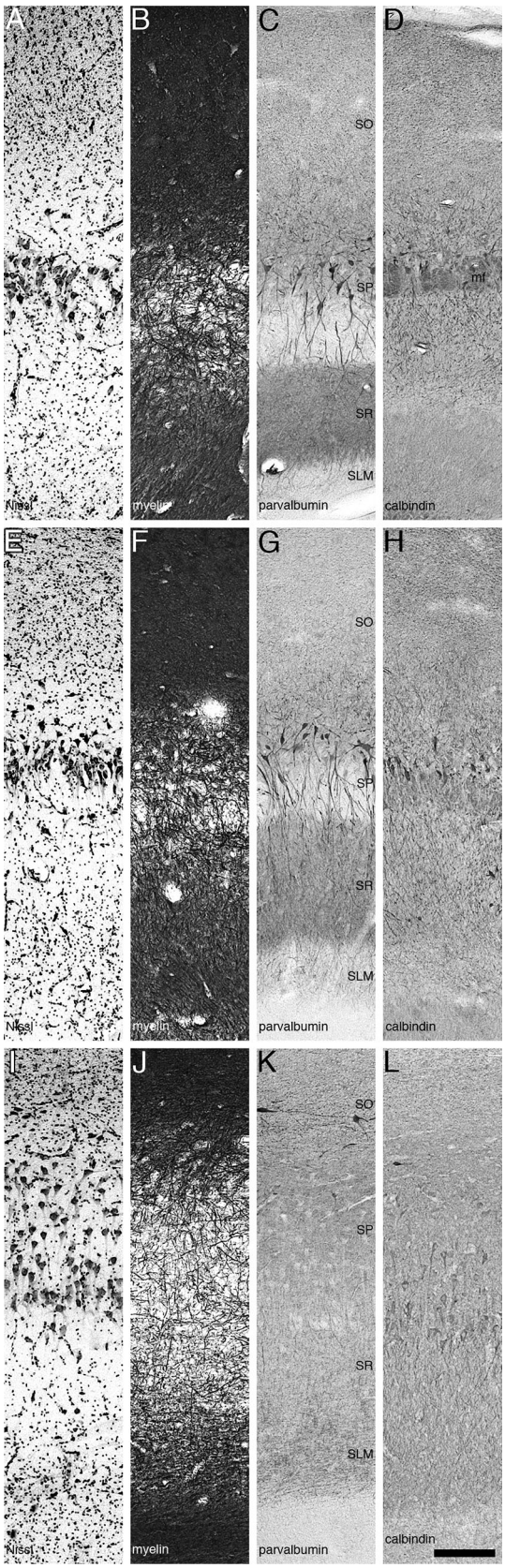

◀**Fig. 6** Higher power photomicrographs of cornu ammonis fields (CA3: **a**–**d**; CA2: **e**–**h**; CA1: **i**–**l**). The cornu ammonis could be subdivided into following strata: stratum oriens (SO), the stratum pyramidale (SP), stratum radiatum (SR) and stratum lacunosum moleculare (SLM). **a**, **e**, **i** Nissl staining revealed a cell dense **SP** and a neuron sparse SO, SR and SLM. The SP was less dense in the CA3 towards the dentate gyrus and became more densely packed towards CA2. In the CA1 field the SP was broader than in CA3 and CA2 and became even more broad at the transition to the subiculum. **b**, **f**, **j** A dense myelinated fibre network was observed in the SO, SR and SLM, with the highest fibre density in the SO. Parvalbumin immunostaining revealed a moderate number of cells in the SP of CA3 (**c**) and CA2 (**g**), but no parvalbumin-immunopositive neurons could be observed in the SP of CA1 (**k**). A few parvalbumin-immunopositive cells were observed in the SO just beneath the SP. The SR could be clearly distinguished by a high parvalbumin-immunopositive terminal network. **d** Calbindin immunostaining revealed mossy fibres (mf) of the granule cells of the DG, located between the SP and SR in the CA3 field. **d**, **h**, **l** A few calbindin-immunopositive cells were observed in the SP and SO just beneath the SP in all fields. *Scale bar* in **l** = 250 μm and applies to all

reporting that the rock hyrax has a very large hippocampus and the Florida manatee a very small hippocampus; however, no quantification supporting these statements is provided. Hakeem et al. (2005) refer to Haug (1970) to support their conclusion of a large hippocampus for the elephant. Haug (1970) provides a hippocampal volume of 29 ± 5 ml for the one elephant hippocampus he measured, which also had small brain mass (4210 g), but he does not provide details as to what exactly is included in his volume analysis of the hippocampus, except to state that the brain was immersion-fixed in formalin for 9 months, and then volumes recalculated based on estimates of what the fresh volumes should be. In this sense, it becomes very unclear as to how Haug (1970) arrived at his measurements especially as details regarding what is considered hippocampus are lacking in his report. A more recent paper by Reep et al. (2007) demonstrates that the volume of the hippocampus of the Florida manatee is what would be expected of a mammal with its brain size. Thus, in both the case of the African elephant and the Florida manatee, when quantification is provided, the statements made by Hakeem et al. (2005) appear to be erroneous. To date, no quantification of the hippocampal volume of the rock hyrax is available to test whether they have a "very large hippocampus", but published observations on the rock hyrax brain suggest that, like the manatee, it will be of the size expected for a mammal with an approximately 16 g brain (see figures in Gravett et al. 2009).

An open question regarding the differences between the Hakeem et al. (2005) study and the current study combined with that of Shoshani et al. (2006), is how the former arrived at the conclusion that the elephant hippocampus was very large. We feel that this conclusion was reached on

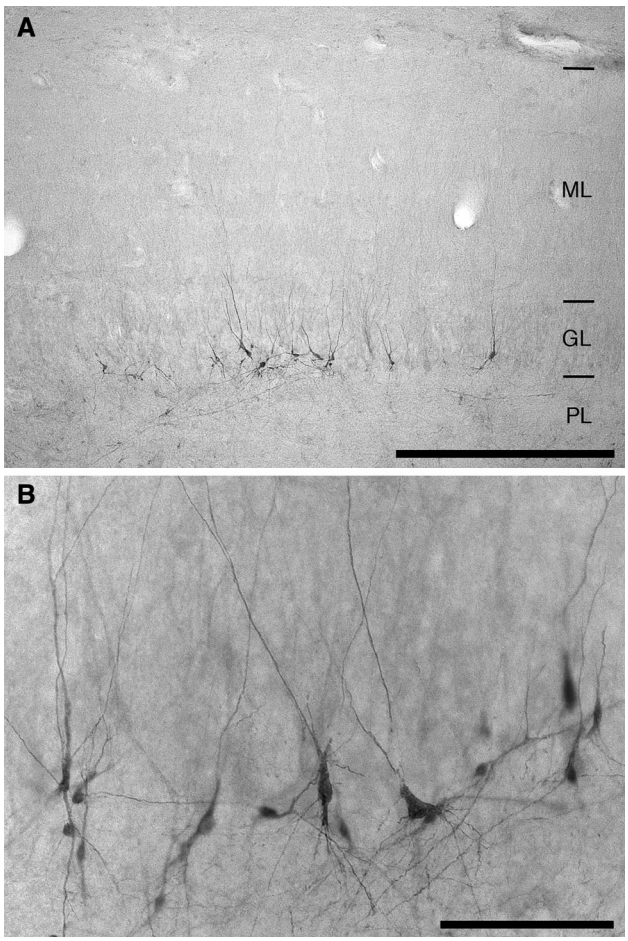

Fig. 7 Higher power photomicrographs of sections immunostained for doublecortin (DCX). A moderate number of DCX-immunopositive cells and processes were observed in the subgranular zone and in the granule cell layer of the dentate gyrus, indicating the generation of new neurons in the hippocampus of adult African elephant. *Scale bar* in **a** = 500 μm and in **b** = 100 μm

the basis of two specific errors. First, Hakeem et al. appear to include a large portion of the occipital pole cortex in their estimation of hippocampal volume (see their Fig. 12A which has no hippocampus in the scan shown). This inclusion of the occipital pole cortex appears to be based on a misreading of their MR images due to the collapse of the ventricular system (compare with the elephant ventricular system shown in Maseko et al. 2011, which demonstrates this problem for the Hakeem et al. specimen). Moreover, Hakeem et al. only show the true hippocampus of the elephant in one slice of their horizontal series (their Fig. 4, Slice 56), which shows a non-convoluted hippocampus, and then mislabel part of the occipital pole cortex as the hippocampus in their Fig. 4 Slices 67 and 74. They do not show a sagittal scan of the hippocampal region, but in their coronal scans (their Fig. 10, slice 260) they label both the dorsal aspect of the hippocampus and the more ventrolaterally located occipital pole cortex as hippocampus. The second error comes from what appears to be the strong influence of the behavioural "neuroecology" paradigm, which intimates that any animal reputed to have a good memory should also have a large hippocampus, based on the careful studies of bird hippocampal volume variations (e.g. Lucas et al. 2004; Healy et al. 2005; Salwiczek et al. 2010). Thus, despite the data generated for the elephant, Hakeem et al. (2005) appear to have had a preconceived idea of what the result should be, based on the behavioural data regarding elephant memory capacities. We feel that it is these two errors that have led to the overestimation of hippocampal volume in the elephant by Hakeem et al. (2005).

Variations in calcium-binding protein expression in the mammalian hippocampus

The present data suggest that the general expression pattern of calcium-binding proteins (parvalbumin, calbindin and calretinin) in the elephant hippocampus is, to some extent, comparable to that seen in mice, rats, dogs, monkeys and humans (Blasco-Ibáñez and Freund 1997; Fujise et al. 1998; Gulyás et al. 1992; Hof et al. 1996; Katsumaru et al. 1988; Liu et al. 1996; Maskey et al. 2012; Nitsch and Ohm 1995; Seress et al. 1991, 2008; Sloviter 1989; Sloviter et al. 1991), although various differences were also observed. In the molecular layer of the dentate gyrus of the elephant, we did not find any neurons immunopositive for the calcium-binding proteins. This is in contrast to other mammals previously studied, where one or more of the calcium-binding proteins were present in one or more different neuronal types. This layer also showed the most striking difference in organization in the elephant when compared to the other mammals, as in the elephant there appears to be two neuropil gradients of calretinin immunostaining (one in the inner and one in the outer molecular layer), whereas in other mammals only the inner molecular layer shows neuropil staining for calretinin, but this is not evinced as a gradient as seen in the elephant. In the mouse it was demonstrated that these are mainly the fibres of calretinin-immunopositive mossy cells of the polymorphic layer, also known as the associational pathway (ASS) (Fujise et al. 1998); whereas studies in rats and humans suggest that the main portion of these calretinin-immunopositive fibres in the iML of the DG originate from the supramammillary region, forming the supramammillary pathway (SUM) (Gulyás et al. 1992; Krzywkowski et al. 1995; Nitsch and Leranth 1993). In contrast to this, in monkeys it was demonstrated that the calretinin-expressing band of the iML receives input from both pathways. The oML, also known as the "entorhinal zone", receives its input mostly from fibres of the entorhinal cortex (layer II stellate neurons), where they innervate the distal dendritic portions of

granule neurons (Deller et al. 1996; Witter 2007). These observations lead to the question—terminals of what pathways are represented in the calretinin-immunopositive bands/gradients of the oML and iML in the elephant? There are several possibilities: (1) the two pathways, associative and suprammallilary are spatially separated, with one projecting onto the iML and the other onto the oML; (2) both pathways project onto both the oMl and iML; (3) the SUM projects onto the oML and iML and the ASS projects either only onto the oML or the iML; or (4) the ASS projects into the iML and oML and the SUM projects either onto the OML or the iML. This observation raises another question—where do the entorhinal fibres terminate in the elephant? Are these terminals integrated with the calretinin-immunopositive terminals in the oML, or do they terminate at the superficial end of the oML and iML where calretinin immunoreactivity diminishes? Tracing studies, using post-mortem tracing techniques such as DiI, would be required to gain a better understanding of the dentate gyrus afferent connectivity patterns in the elephant hippocampus. Irrespective of these four possibilities, it appears that the organization of the molecular layer of the elephant is clearly different to that seen in other mammals, and may even be thought of as more complexly organized. This likely has a strong effect on the manner in which the dendritic potentials of the apical dendrites of the granule cells process information locally.

Virtually all granule cells, the principal neurons of the dentate gyrus, and their unmyelinated axons which project as mossy fibres to CA3, are calbindin-immunopositive and this appears to be a common feature of mammals surveyed to date (Maskey et al. 2012; Seress et al. 1991; Hof et al. 1996; Sloviter 1989; Sloviter et al. 1991) including the elephant. In rodents and primates, there are a few calretinin- and parvalbumin-immunopositive neurons present in the granule layer (Maskey et al. 2012; Liu et al. 1996; Nitsch and Ohm 1995; Seress et al. 2008; Sloviter 1989; Sloviter et al. 1991). These were not present in the elephant, and they have also not been reported in the dog (Hof et al. 1996). In the polymorphic layer of the elephant, we only found evidence for calretinin-immunopositive neurons (presumably mossy cells), and this appears to be a common feature among the mammals surveyed to the exception of the rat (Liu et al. 1996). No calbindin- or parvalbumin-immunopositive neurons were observed in the polymorphic layer of the elephant, but these have been observed in several other mammals (Hof et al. 1996; Maskey et al. 2012; Liu et al. 1996; Nitsch and Ohm 1995; Seress et al. 2008; Sloviter 1989; Sloviter et al. 1991). As with the other mammals, fibres and terminal networks immunoreactive to all three calcium-binding proteins were observed in the polymorphic layer of the elephant dentate gyrus.

Another common feature of all mammals surveyed, including the elephant, was the presence of parvalbumin-immunopositive cells in the SP of the CA3 and CA2 fields. These cells are reported to be large and multipolar, with their basal dendrites extending into the SO and the apical dendrite into SR and SLM. In addition, CA1 fusiform, horizontally orientated cells just below the SP in the SO, immunoreactive for all three calcium-binding proteins, were present in almost all mammals surveyed, including the elephant. Such a comparable morphology and similar location of these neurons between different species of distinct phylogenetic lineages indicates that these cells might be involved in similar microcircuitry in the hippocampus (Hof et al. 1996).

The remaining layers of the different CA fields, showed a great deal of variance in the expression patterns of the calcium-binding proteins. Taken together, these results suggest that cells with similar morphology and neurochemistry probably represent similar neuronal populations with similar functions between different species within the hippocampal circuitry (Hof et al. 1996). Calcium-binding proteins have been demonstrated to play an important role in modulating intracellular calcium dynamics in neurons (Baimbridge et al. 1992; Barinka and Druga 2010; Caillard et al. 2000). Parvalbumin is a slow Ca^{2+} buffer, calbindin has a faster Ca^{2+} buffering rate than parvalbumin, whereas calretinin seems to accelerate the binding rate, as it binds more Ca^{2+} and therefore has the properties of a slow and fast buffer (Faas et al. 2007; Barinka and Druga 2010). Although the exact effects that the expression complement of calcium-binding proteins may have on the hippocampal circuitry in the elephant, or other mammals, are unknown, these are likely to be significant. It would be of interest to undertake a broad comparative survey of the expression of these proteins across mammalian species (e.g. Hof et al. 1999), both within and between orders, to determine whether there is a phylogenetic signal in their expression within the circuitry, and if the differences between species provide some predictability of the computational outcomes of hippocampal activity.

Neurogenesis in the adult mammalian hippocampus

The mammalian hippocampus is known as one of the two regions in which generation of new neurons occurs throughout life (Kempermann 2012). The cells are born in the subgranular zone of the dentate gyrus, from where they migrate into the granule cell layer and become functionally integrated into the dentate gyrus circuitry (Ming and Song 2011; Lindsey and Tropepe 2006; Gould 2007). Evidence suggestive of adult neurogenesis in the dentate gyrus of the elephant was provided by immunostaining for doublecortin (DCX). A moderate density of DCX-immunoreactive cells

was observed in the subgranular zone and granule layer with their dendrites projecting into the inner molecular layer of the dentate gyrus, representing a pattern of neurogenesis typically observed in other mammals. To date most of the studies on adult hippocampal neurogenesis have been carried out on laboratory rodents (Bonfanti et al. 2011) and only a few other mammalian species have been analyzed (Kempermann 2012). Nevertheless it appears that adult hippocampal neurogenesis is a common feature of mammals. The current study indicates the addition of another species to the list of animals analyzed to date where adult hippocampal neurogenesis has been observed.

The hippocampus and life history of the African elephant

As mentioned earlier, the African elephant appears to have complex spatial–temporal and social memory capacities that are not readily observed in other mammals; however, the observations regarding the memory capacities of elephants have been popularized to such an extent that the elephant memory has become folkloric and has led to speculation. The data presented in the current study can be used to contextualize the memory capacities of the elephant from a more pragmatic viewpoint and one that might be more useful to our long-term understanding in terms of management and conservation of the species. First, for the most part, the histological structure of the elephant hippocampus, including the presence of adult hippocampal neurogenesis, does not differ dramatically from that seen in other mammals, the one exception being the complex lamination of the molecular layer of the dentate gyrus (discussed above). Second, the size of the elephant hippocampus is not much larger in absolute size than that observed for the human hippocampus, despite the human having a significantly smaller overall brain size. Thus, in a generalized sense, the processing of neural information in the elephant hippocampus cannot be considered at present to be especially different from that seen in other mammals including humans. While differences such as the complex sublamination of the molecular layer of the dentate gyrus may augment specific aspects of neural information processing, it would be hard to imagine that this would lead to more developed memory processing capabilities compared to other mammals. The absolute size of the elephant hippocampus also argues towards this interpretation. Given that larger brains, or regions within the brain, appear to have more complex neurons (e.g. Maseko et al. 2013), it is also possible that in comparison with most other mammals, the individual neuronal elements of the elephant hippocampus may be more complexly organized than that of other mammals, in terms of dendritic field size, branching complexity and spine numbers, except for perhaps the human. This then may indicate that the hippocampal neuronal information processing in elephants is likely to be similar in complexity to that seen in humans, but may be more complex than seen in other mammals.

Like the human, elephants are long-lived terrestrial mammals. In this sense, the complexity and capacity for the generation and recall of episodic and autobiographical memories are likely to be similar between the two species. This is substantiated by the overall similarities in size and structure of the hippocampal formation in the two species. Thus, we feel it is most pragmatic to conclude that the memory capacities, in terms of formation, recall, utilization and clarity, of the elephant and human are likely to be similar. This would fit well with the fact that both these terrestrial mammalian species need to form and recall memories throughout a reasonably long life span to ensure survival in terms of spatial–temporal and social aspects of their life histories. We, therefore, conclude that the memory systems of the elephants are probably very similar to that of humans, perhaps more complex than that of other mammals, but no more complex than would be expected for a terrestrial mammal with a long life span and a social lifestyle.

Acknowledgments This study was supported by a grant from the South African National Research Foundation to PRM (Grant number: FA2005033100004), the Swiss-South African Joint Research Programme to AOI and PRM, a fellowship within the Postdoc-Programme of the German Academic Exchange Service, DAAD (NP), and the James S. McDonnell Foundation (Grant 22002078 to PRH). We would like to thank Dr. Hilary Madzikanda of the Zimbabwe Parks and Wildlife Management Authority, and Dr. Bruce Fivaz and the team at the Malilangwe Trust, Zimbabwe.

Conflict of interest The authors have no conflict of interest.

References

Baimbridge KG, Celio MR, Rogers JH (1992) Calcium-binding proteins in the nervous system. Trends Neurosci 15:303–308

Barinka F, Druga R (2010) Calretinin expression in the mammalian neocortex: a review. Physiol Rev 59:665–677

Bartkowska K, Turlejski K, Grabiec M, Ghazaryan A, Yavruoyan E, Djavadian RL (2010) Adult neurogenesis in the hedgehog (*Erinaceus concolor*) and mole (*Talpa europaea*). Brain Behav Evol 76:128–143

Bates LA, Sayialel KN, Njiraini N, Poole JH, Moss C, Byrne RW (2008) African elephants have expectations about the locations of out-of-sight family members. Biol Lett 4:34–36

Blasco-Ibáñez JM, Freund TF (1997) Distribution, ultrastructure, and connectivity of calretinin-immunoreactive mossy cells of the mouse dentate gyrus. Hippocampus 7:307–320

Bonfanti L, Rossi F, Zupanc GK (2011) Towards a comparative understanding of adult neurogenesis. Eur J Neurosci 34:845–846

Brown JP, Couillard-Despres S, Cooper-Kuhn CM, Winkler J, Aigner L, Kuhn HG (2003) Transient expression of doublecortin during adult neurogenesis. J Comp Neurol 467:1–10

Byrne RW, Bates LA, Moss CJ (2009) Elephant cognition in primate perspective. Comp Cog Behav Rev 4:1–15

Caillard O, Moreno H, Schwaller B, Llano I, Celio MR, Marty A (2000) Role of the calcium-binding protein parvalbumin in short-term synaptic plasticity. Proc Natl Acad Sci USA 97: 13372–13377

Deller T, Adelmann G, Nitsch R, Frotscher M (1996) The alvear pathway of the rat hippocampus. Cell Tissue Res 286:293–303

Faas GC, Schwaller B, Vergara JL, Mody I (2007) Resolving the fast kinetics of cooperative binding: Ca^{2+} buffering by calretinin. PLoS Biol 5:e311

Foley CAH, Pettorelli N, Foley L (2008) Severe drought and calf survival in elephants. Biol Lett 4:541–544

Fujise N, Liu Y, Hori N, Kosaka T (1998) Distribution of calretinin immunoreactivity in the mouse dentate gyrus: II. Mossy cells, with special reference to their dorsoventral difference in calretinin immunoreactivity. Neuroscience 82:181–200

Gallyas F (1979) Silver staining of myelin by means of physical development. Neurol Res 1:203–209

Gould E (2007) How widespread is adult neurogenesis in mammals? Nat Rev Neurosci 8:481–488

Gravett N, Bhagwandin A, Fuxe K, Manger PR (2009) Nuclear organization and morphology of cholinergic, putative catecholaminergic and serotonergic neurons in the brain of the rock hyrax, *Procavia capensis*. J Chem Neuroanat 38:57–74

Gulyás AI, Miettinen R, Jacobowitz DM, Freund TF (1992) Calretinin is present in non-pyramidal cells of the rat hippocampus-I. A new type of neuron specifically associated with the mossy fiber system. Neuroscience 48:1–27

Hakeem AY, Hof PR, Sherwood CC, Switzer RC, Rasmussen LE, Allman JM (2005) Brain of the African elephant (*Loxodonta africana*): neuroanatomy from magnetic resonance images. Anat Rec 287:1117–1127

Hart BL, Hart LA, Pinter-Wollman N (2008) Large brains and cognition: where do elephants fit in? Neurosci Biobehav Rev 32:86–98

Haug H (1970) Der makroskopische Aufbau des Grosshirns; Qualitative und quantitative Untersuchungen an den Gehirnen des Menschen, der Delphinoideae und des Elefanten. Ergebn Anat Entwicklungesch 43:3–70

Healy SD, de Kort SR, Clayton NS (2005) The hippocampus spatial memory and food hoarding: a puzzle revisited. Trends Ecol Evol 20:17–22

Hof PR, Rosenthal RE, Fiskum G (1996) Distribution of neurofilament protein and calcium-binding proteins parvalbumin, calbindin, and calretinin in the canine hippocampus. J Chem Neuroanat 11:1–12

Hof PR, Glezer II, Conde F, Flagg RA, Rubin MB, Nimchinsky EA, Vogt Weisenhorn DM (1999) Cellular distribution of the calcium-binding proteins parvalbumin, calbindin, and calretinin in the neocortex of mammals: phylogenetic and developmental patterns. J Chem Neuroanat 16:77–116

Katsumaru H, Kosaka T, Heizmann CW, Hama K (1988) Immunocytochemical study of GABAergic neurons containing the calcium-binding protein parvalbumin in the rat hippocampus. Exp Brain Res 72:347–362

Kempermann G (2012) New neurons for 'survival of the fittest'. Nat Rev Neurosci 13:727–736

Krzywkowski P, Jacobowitz DM, Lamour Y (1995) Calretinin-containing pathways in the rat forebrain. Brain Res 705:273–294

Kupsky WJ, Marchant GH, Cook K, Shoshani J (2001) Morphologic analysis of the hippocampal formation in *Elephas maximus* and *Loxodonta africana* with comparison to that of human. In: Cavarretta G, Gioia P, Mussi M, Palombo MR (eds) Proceedings of the 1st International Congress of "La Terra degli Elefanti", The World of Elephants. Consiglio Nazionale delle Ricerche, Roma, pp 643–647

Lindsey BW, Tropepe V (2006) A comparative framework for understanding the biological principles of adult neurogenesis. Prog Neurobiol 80:281–307

Liu Y, Fujise N, Kosaka T (1996) Distribution of calretinin immunoreactivity in the mouse dentate gyrus. I. General description. Exp Brain Res 108:389–403

Lucas JR, Brodin A, de Kort SR, Clayton NS (2004) Does hippocampal size correlate with degree of caching specialization? Proc Biol Sci 271:2423–2429

Manger PR, Pillay P, Maseko BC, Bhagwandin A, Gravett N, Moon D, Jillani NE, Hemingway J (2009) Acquisition of the brain of the African elephant (*Loxodonta africana*): perfusion-fixation and dissection. J Neurosci Methods 179:16–21

Maseko BC, Spocter MA, Haagensen M, Manger PR (2011) Volumetric analysis of the African elephant ventricular system. Anat Rec 298:1412–1417

Maseko BC, Jacobs B, Spocter MA, Sherwood CC, Hof PR, Manger PR (2013) Qualitative and quantitative aspects of the microanatomy of the African elephant cerebellar cortex. Brain Behav Evol 81:40–55

Maskey D, Pradhan J, Oh CK, Kim MJ (2012) Changes in the distribution of calbindin D28-k, parvalbumin, and calretinin in the hippocampus of the circling mouse. Brain Res 1437:58–68

McComb K, Moss C, Sayailel S, Baker L (2000) Unusually extensive networks of vocal recognition in African elephants. Anim Behav 59:1103–1109

McComb K, Reby D, Baker L, Moss C, Sayailel S (2003) Longdistance communication of acoustic cues to social identity in African elephants. Anim Behav 65:317–329

Ming GL, Song H (2011) Adult neurogenesis in the mammalian brain: significant answers and significant questions. Neuron 70: 687–702

Morris R (2007) Theories of hippocampal function. In: Anderson P, Morris R, Amaral D, Bliss T, O'Keefe J (eds) The Hippocampus Book. Oxford Press, New York, pp 581–715

Ngwenya A, Patzke N, Ihunwo AO, Manger PR (2011) Organisation and chemical neuroanatomy of the African elephant (*Loxodonta africana*) olfactory bulb. Brain Struct Funct 216:403–416

Nitsch R, Leranth C (1993) Calretinin immunoreactivity in the monkey hippocampal formation-II. Intrinsic GABAergic and hypothalamic non-GABAergic systems: an experimental tracing and co-existence study. Neuroscience 55:797–812

Nitsch R, Ohm TG (1995) Calretinin immunoreactive structures in the human hippocampal formation. J Comp Neurol 360:475–487

Poole JH, Payne K, Langbauer WR, Moss CJ (1988) The social contexts of some very low frequency calls of African elephants. Behav Ecol Sociobiol 22:385–392

Quiroga RQ, Reddy L, Kreiman G, Koch C, Fried I (2005) Invariant visual representation by single neurons in the human brain. Nature 435:1102–1107

Rao MS, Shetty AK (2004) Efficacy of doublecortin as a marker to analyse the absolute number and dendritic growth of newly generated neurons in the adult dentate gyrus. Eur J Neurosci 19:234–246

Reep RL, Finlay BL, Darlington RB (2007) The limbic system in mammalian brain evolution. Brain Behav Evol 70:57–70

Rosset A, Spadola L, Ratib O (2004) OsiriX: an open-source software for navigating in multidimensional DICOM images. J Digit Imaging 17:205–216

Salwiczek LH, Watanabe A, Clayton NS (2010) Ten years of research into avian models of episodic-like memory and its implications for developmental and comparative cognition. Behav Brain Res 215:221–234

Seress L, Gulyás AI, Freund TF (1991) Parvalbumin- and calbindin D28k-immunoreactive neurons in the hippocampal formation of the macaque monkey. J Comp Neurol 313:162–177

Seress L, Abrahám H, Czéh B, Fuchs E, Léránth C (2008) Calretinin expression in hilar mossy cells of the hippocampal dentate gyrus of nonhuman primates and humans. Hippocampus 18:425–434

Shoshani J, Kupsky WJ, Marchant GH (2006) Elephant brain. Part I: gross morphology, functions, comparative anatomy, and evolution. Brain Res Bull 70:124–157

Skinner JD, Chimimba CT (2005) The Mammals of the Southern African Subregion, 3rd edn. Cambridge University Press, Cape Town

Sloviter RS (1989) Calcium-binding protein (calbindin-D28k) and parvalbumin immunocytochemistry: localization in the rat hippocampus with specific reference to the selective vulnerability of hippocampal neurons to seizure activity. J Comp Neurol 280:183–196

Sloviter RS, Sollas AL, Barbaro NM, Laxer KD (1991) Calcium-binding protein (calbindin-D28K) and parvalbumin immunocytochemistry in the normal and epileptic human hippocampus. J Comp Neurol 308:381–396

Stephan H, Frahm H, Baron G (1981) New and revised data on volumes of brain structures in insectivores and primates. Folia Primatol 35:1–29

Vidya TNC, Sukumar R (2005) Social and reproductive behaviour in elephants. Curr Sci 89:1200–1207

von Heimendahl M, Rao RP, Brecht M (2012) Weak and nondiscriminative responses to conspecifics in the rat hippocampus. J Neurosci 32:2129–2141

Watson C, Andermann F, Gloor P, Jones-Gotman M, Peters T, Evans A, Olivier A, Melanson D, Leroux G (1992) Anatomic basis of amygdaloid and hippocampal volume measurement by magnetic resonance imaging. Neurology 42:1743–1750

Western D, Lindsay WK (1984) Seasonal herd dynamics of a savanna elephant population. Afr J Ecol 22:229–244

Witter MP (2007) The perforant path: projections from the entorhinal cortex to the dentate gyrus. Prog Brain Res 163:43–61